Advanced Materials Research *Online: 2014-08-11*
ISSN: 1662-8985, Vol. 996, pp 500-505
doi:10.4028/www.scientific.net/AMR.996.500

Residual stresses of explosion cladded composite plates of ZERON 100 superduplex stainless steel and ASTM SA516-70 carbon steel

Rogério Varavallo[1,a], Vitor de Melo Moreira[1,b], Vinicius Paes[1,c], Pedro Brito[2,d], Jose Olivas[3,e] and Haroldo Cavalcanti Pinto*[1,f]

[1]Universidade de São Paulo, Av. Trabalhador São Carlense 400, 13566-590 São Carlos SP, Brazil.

[2]Pontifícia Universidade Católica de Minas Gerais, Av. Dom José Gaspar 500, 30535-901 Belo Horizonte MG, Brazil.

[3]Dynamic Materials Corporation, 5405 Spine Road, Boulder, CO 80301, United States.

[a]roger_varavallo@yahoo.com.br, [b]vitor.s.melo@hotmail.com, [c]vinipaes@hotmail.com, [d]pbrito@pucminas.br, [e]JOlivas@dynamicmaterials.com, [f]haroldo@sc.usp.br

*Corresponding author.

Keywords: Explosion cladding, superduplex stainless steel, heat treatment, residual stress.

Abstract. In the present work bimetal composite plates of ZERON 100 superduplex stainless steel and ASME SA516-70 carbon steel were produced by explosion welding and submitted to post weld heat treatment for stress relief. The cross section microstructure of the cladded plates was characterized by optical microscopy and scanning electron microscopy and the hardness profile across the weld interface was determined. Residual stress analysis by X-ray diffraction was performed before and after heat treatment on the stainless steel side of the cladded plates. In the as-welded condition, metallography analysis indicated severe plastic deformation at the welded interface and a wavy morphology characteristic of high adhesive strength. Elevated tensile residual stresses were created as a result of the welding process. The heat treatment process applied (6h at 250°C) did not alter hardness at the welded interface nor the residual stress state in the cladded materials.

1. Introduction

Low carbon steels are excellent materials for structural applications. They possess high strength, are inexpensive, readily available, present good formability and can be easily welded. However, due to their poor corrosion resistance, they cannot be selected for structures designed to operate in highly corrosive environments, such as offshore applications. On the other hand, the selection of bulk corrosion resistant materials, while technically effective, may lead to significant increases in cost. A common circumvention to this problem is to apply composite materials, whereby a high cost corrosion resistant metal, e.g. stainless steel, is cladded onto a less expensive carbon steel substrate thus combining adequate properties with an affordable price [1].

Explosion welding is a solid state joining technique developed in the mid-1950s [2] largely employed for manufacturing composite metal plates where conventional fusion welding processes would be impractical [3]. The metal plates are initially fixed parallel to each other separated by a predetermined standoff distance. An explosive is placed on top of the flyer plate (or clad metal). Upon detonation of the explosive, the flyer plate is accelerated and strikes the base plate resulting in an intense oblique collision. Upon impact a high velocity jet is formed, sweeping away surface impurities and assisting the establishment of a metallurgical bond [4]. The bond involves plastic deformation in both metals and may result in a wavy interface [2, 5].

While explosion welding is considered a solid state process, dissipation of the elevated impact energy can increase temperatures at the interface causing local melting and/or annealing of the base materials [6]. Because the heating is highly concentrated, fast cooling rates ensue which may lead to the formation of very fine grains near the welding interface [7]. This means that metallurgical transformations and diffusion processes are restricted to the cladded interface and explosion welding processes introduce little or no modifications in the properties of the base materials themselves. In addition, joining of dissimilar materials by explosion welding does not give rise to intermetallic compounds [4] and is more easily achieved in comparison to conventional fusion welding processes.

The cladded materials produced by explosion welding are not, however, free of residual stresses also common for fusion welding processes. In explosion welding, residual stresses may be caused by intense plastic deformation at the interface, differences in material properties and sharp temperature gradients. Welding induced residual stresses may cause e.g. dimensional instability during cutting or machining operations and explosion welding residual stresses have been recently explored [7-10]. In the present work, an investigation of the microstructure and residual stresses formed as a consequence of the explosion welding process applied to the production of composite plates of ASME SA516-70 carbon steel and ZERON 100 (UNS S32760) superduplex stainless steel is proposed. The objective of this analysis is to provide explanations regarding the origins of residual stresses in this particular joint. Characterization of the microstrucutre formed after application of a post weld heat treatment for stress relexation was also carried out.

2. Experimental Procedure

Materials. Plates of ASME SA516-70 carbon steel and ZERON 100 superduplex stainless steel were explosion welded in parallel configuration (nominal chemical composition of both steels is given in Table 1). The composite plates were produced in parallel configuration with the ASME SA516-70 steel being the base plate and the ZERON 100 stainless steel being the clad metal or flyer plate. Prior to welding, both steel plates were inspected for surface defects and ground in order to increase effective contact area and assist the bonding process. The final dimensions of the composite plates were 762x330x31.6 mm. The welding procedures were carried out by Dynamic Materials Corporation (US).

Table 1. Nominal chemical composition of the SA516-70 and ZERON 100 steels (values in wt.%)

Steel	C	Si	Mn	Al	Cr	Cu	Ni	Mo	Nb	Ti	V	W	N
SA516-70	0.1-0.22	0.6	1-1.7	0.02	0.3	0.3	0.3	0.08	0.01	0.03	0.02	-	-
ZERON 100	0.03	1.0	1.0	-	24.0-26.0	0.5-1.0	6.0-8.0	3.0-4.0	-	-	-	0.5-1.0	0.2-0.3

Stress relief heat treatment. Post weld heat treatment for stress relief was carried out in a conventional furnace (with no controlled atmosphere) at 250°C for 6 h. After annealing, the samples were removed from the furnace and air-cooled. The temperature was selected in order to minimize microstructure modifications (e. g. grain growth, phase transformations) of both materials.

Microstructure analysis. Samples for microstructure analysis were prepared by applying mechanical grinding with 80 to 1200 grit SiC grinding paper followed by polishing in 6 and 3 μm diamond suspensions. Behara's reagent (20 ml HCL, 80 ml distilled water and 1 g $K_2S_2O_5$) was used for etching the ZERON 100 stainless steel while a 2% Nital solution was used for etching the SA516-70 carbon steel. Observation of the microstructure was performed by applying Optical Microscopy (OM), Scanning Electron Microscopy (SEM) and Energy-Dispersive X-ray spectroscopy (EDX).

Microhardness measurements. Vickers microhardness measurements were performed across the cladded interface with a 100 gf load (HV0.1) in 0.2 mm steps with a 15 s holding time. In total, three microhardness profiles were measured and the average values were determined. The hardness of the original base materials before application of the welding procedure was also determined.

Residual stress analysis. Residual stress analysis was performed by X-ray Diffraction (XRD) on a 60x60x20 mm piece which was carefully sectioned and removed from the original welded materials. The cladded plate had to be thinned in order to properly fit the diffractometer and the excess material was removed from the SA516-70 steel side of the plate. No other procedures were performed on the cladded materials prior to residual stress determination. The $\sin^2\psi$ method was used with equally spaced ψ intervals between 0 and 71.57°, in two azimuthal (φ) directions (0 and 180°). The measurements were performed on the ZERON 100 steel side of the cladded plate by analyzing the reflections from the ferrite (211) and austenite (311) lattice planes. A laboratory Co K_α source was used in the experiments with the X-ray beam focused on the center of the 60x60 mm surface of the ZERON 100 plate. The distance from the investigated surface to the cladded interface itself was of 5 mm. Using Co K_α with the selected diffraction lines yields an information depth of about 60 µm. The values of the elastic constants were S_1 = -1.558 MPa^{-1} and $½S_2$ = 7.005 MPa^{-1} for the (311) austenite reflection and S_1 = -1.268 MPa^{-1} and $½S_2$ = 5.804 MPa^{-1} for the (211) ferrite reflection. The 60x60x20 plate was positioned in the diffractometer so that its surface normal corresponded to $\psi = 0°$ while the cladded interface corresponded to $\psi = 90°$.

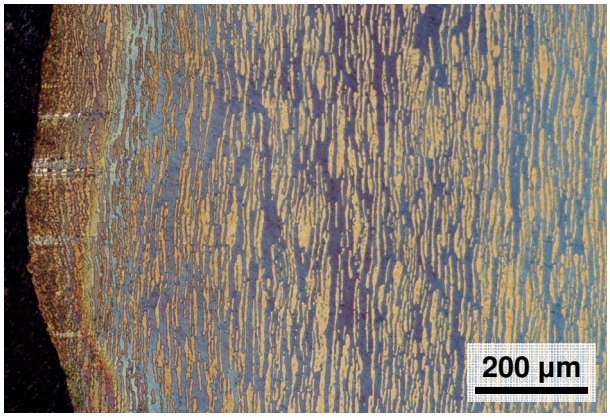

Figure 1: Optical micrograph from the as welded ZERON 100 steel (Behara's etchant)

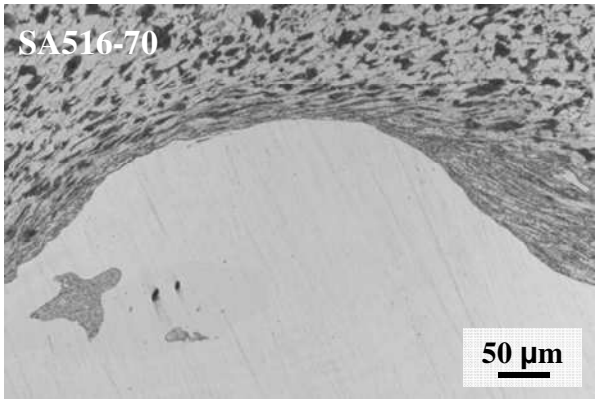

Figure 2: Optical micrograph from the SA516-70 steel side of the cladded interface, in the as welded condition (Nital 2% etchant).

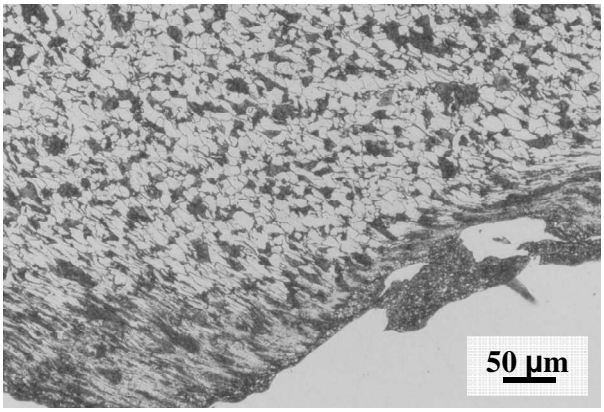

Figure 3: Optical micrograph of the SA516-70 side of the cladded interface obtained after heat treatment at 250 °C for 6 h.

3. Results and Discussion

Microstructure. OM micrographs of the as welded ZERON 100 and SA516-70 steels are presented in Fig. 1 and 2, respectively. The microstructure of the ZERON 100 base material consists of alternating layers of elongated ferrite and austenite grains. It is clear that the microstructure changes significantly close to the cladded interface with the layers of ferrite and austenite grains becoming thinner and more compact. In Fig. 2 the wavy interface, characteristic of explosion welding processes [2, 5], can be clearly visualized. The SA516-70 base material is formed by equiaxed ferrite grains and pearlite colonies which close to the interface (50-100 µm) become elongated parallel to the impact direction. The near interface region of both materials exhibits clear

signs of severe plastic deformation. The microstructure of the cladded interface obtained after heat treatment at 250 °C for 6 h was also analyzed by optical microscopy and the results are presented Fig. 3. Under the same magnification which was used for Fig. 2, no significant changes in grain morphology can be visualized after the proposed heat treatment.

The cladded interface of the as welded material was further analyzed by SEM and the result is presented in Fig. 4. Chemical composition line profile analysis was performed across the interface by EDX at the position indicated by the dotted line, and the results are also presented in Fig. 4. The higher contrast of the electron microscope reveals the presence of a transition region between the base materials. This particle has an intermediate chemical composition relative to the ZERON 100 and S516-70 steels, noticeably in terms of Cr and Fe concentration, as can be seen in Fig. 5. The Fe concentration in the SA516-70 base material is of close to 92%, reaches an average 88% in the intermediate region near the interface and, finally, in the ZERON 100 base material is 59%. On the other hand, Cr concentration is negligible on the SA516-70 steel, rises to an average 6% near the interface and, finally, reaches 26% in the ZERON 100 steel. This variation of chemical composition across the cladded interface is probably an indication of localized melting and mixing of the SA516-70 and ZERON 100 steels [11]. It is important to notice that the particle does not form a continuous layer along the remainder of the interface, which is sharp instead.

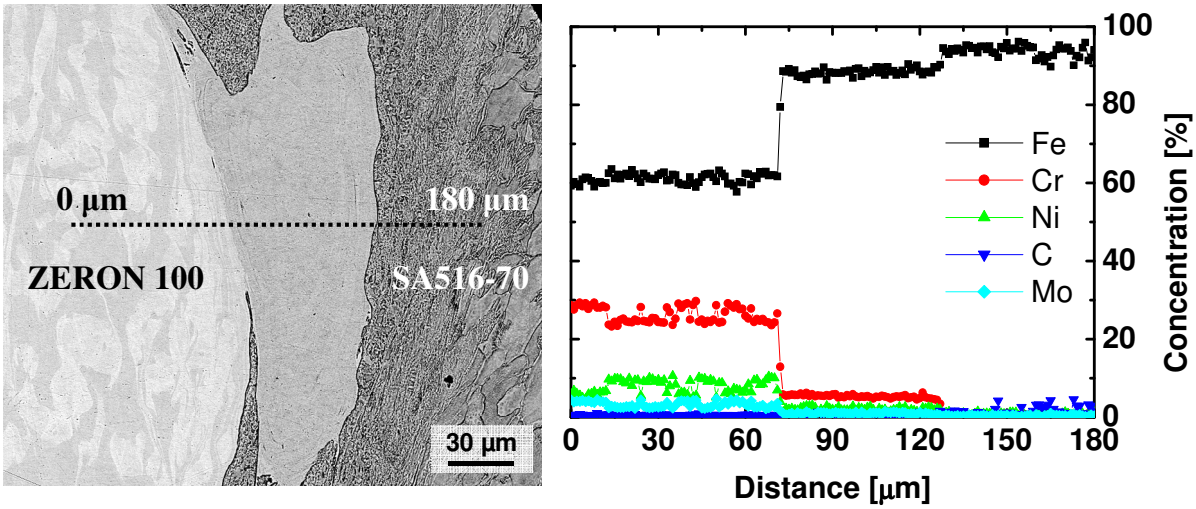

Figure 4: SEM micrograph of the cladded interface EDX chemical composition profile.

Microhardness. The results of the Vickers hardness profiles measured across the cladded interface for the as welded and heat treated conditions are presented in Fig. 5. The hardness values of the base materials prior to the welding process, indicated by the dashed lines, were 197 and 277HV for the SA516-70 and ZERON 100 steels, respectively. For the as welded condition, the maximum hardness value (467HV) occurs at the bond interface on the ZERON 100 stainless steel side, expected because it is the harder material and strain hardening is more pronounced at the interface. The hardness profile remains unchanged after heat treatment. The maximum hardness value (456HV, similar to the as welded condition) also occurred at the interface.

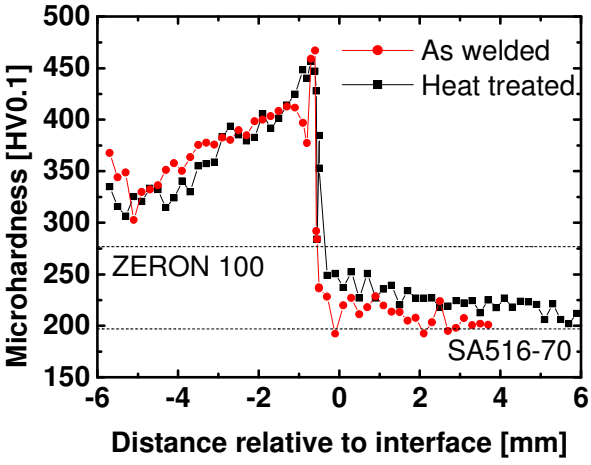

Figure 5: Vickers hardness profiles measured across the cladded interface.

Residual stress analysis. Residual stress analysis was performed on the ZERON 100 stainless steel side of the welded joints in the as welded and heat treated conditions. The plots of the measured the ferrite (200) and austenite (311) lattice distances versus $\sin^2\psi$ are presented in Fig. 6(a) and 6(b) for the as welded condition and heat treated condition, respectively. The residual stress values calculated from the slope of the linear fit of the $\sin^2\psi$ plots were 190±30MPa and 600±50MPa for the ferrite and austenite phases, respectively, for the as welded plate. Because the ZERON 100 steel possesses a dual phase microstructure, with approximately equal amounts of ferrite and austenite grains, it can be considered a composite material and thus the residual stresses determined experimentally for each phase are, in fact, a superposition of macro- and micro-stresses [12]. Welding induced residual stresses are normally caused by inhomogeneous temperature distributions. Close to the bond interface, temperatures are significantly higher relative to the base materials such that, during cooling, the regions near the interface tend to contract while being hindered by the surrounding colder parent material. This leads to tensile stresses directly at the weld joint and balancing compressive residual stresses throughout the base material [13]. The residual stresses associated with welding of different materials (with similar stiffness) are often further connected to differences in the Coefficient of Thermal Expansion (CTE) among the two base materials [9]. It is likely, therefore, that macro-stresses intensify due to CTE mismatch between the ZERON 100 and SA516-70 steel whereas micro-stresses in the ZERON 100 steel result due to the CTE mismatch between austenite and ferrite. In general, ferrite has a lower CTE compared to austenite [14]. Thus, the austenite phase undergoes a larger expansion upon heating in comparison to ferrite, and is left in higher tensile state after cooling down to room temperature, following the explanations of Fitzpatrick and co-workers [12], who calculated thermal micro-stresses in Al-SiC composites. It is worth noticing that the explosion welding process involves intensive plastic deformation near the interface. This may lead, along with the wavy morphology of the interface, to an inhomogeneous strain distribution along the workpiece, thus providing another mechanism for residual stress formation [13].

After heat treatment, the residual stress values for ferrite and austenite were 210±20MPa and 600±50MPa, respectively, as shown in Fig. 6(b). No statistically relevant change in residual stresses could be detected with post-weld annealing, in agreement with the results presented in Fig. 5 which did not indicate significant changes in microstructure before and after heat treatment. It is likely that an increase in heat treatment temperature would be necessary for effective stress relief to take place.

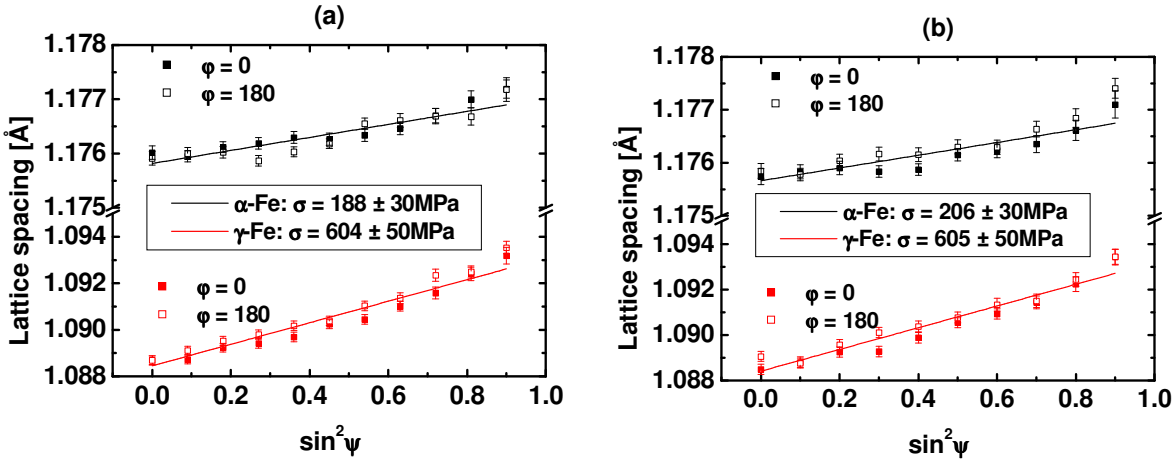

Figure 6: Results of the residual stress analysis performed on the ZERON 100 side of the cladded plate in the (a) as welded condition and (b) after annealing at 250 °C for 6 h.

4. Conclusions

Composite cladded plates of SA516-70 carbon steel and ZERON 100 stainless steel were produced by explosion welding and submitted to post-weld heat treatment. Microstructure analysis of the cladded interface revealed the presence of a wavy morphology characteristic of elevated bond

strength. Localized melted zones could also be identified in the vicinities of the cladded interface which did not, however, amount to a continuous layer. Both materials exhibited signs of intensive plastic deformation near the interface, which produced maximum hardness values of 467HV. The low heat treatment temperature applied was insufficient for recrystallization and hardness was unaffected. Residual stress analysis was performed on the ZERON 100 side of the composite plates. Tensile residual stresses were introduced by the welding process which did not relax after application of post-weld annealing. The residual stresses in austenite were significantly higher in comparison to ferrite, possibly due to differences in thermal expansion between the two phases.

Acknowledgment

The authors express their gratitude towards the Brazilian national council for scientific and technological development (CNPq), University of São Paulo (USP) and the laboratory staff.

References

[1] D.R. Leuser, C.K. Syn, O.D. Sherby, J. Wadsworth, J. J., Lewandowski, W. H. Hunt Jr., Mechanical behaviour of laminated metal composites, Int. Mater. Rev. 41 (1996) 169-197.
[2] A.S. Bahrani, T.J. Black, B. Crossland, The mechanics of wave formation in explosive welding, P. Roy. Soc. Lond. A Mat. 296, 1967, 224-239.
[3] S.A.A. Akbari-Mousavi, L.M. Barrett, S.T.S. Al-Hassani, Explosive welding of metal plates, J. Mater. Process. Tech. 202 (2008) 224-239.
[4] R.A. Patterson, Fundamentals of Explosion Welding, in: D. L. Olson, T. A. Siewert, S. Liu, G. R. Edwards (Eds.), ASM Handbook: Volume 6: Welding Brazing and Soldering, ASM International, Ohio, 1993.
[5] S.A.A. Akbari-Mousavi, S.T.S. Al-Hassani, Numerical and experimental studies of the mechanism of the wavy interface formations in explosive/impact welding, J. Mech. Phys. Solids 53 (2005) 2501-2528.
[6] M. Acarer, B. Gülenç, F. Findik, Investigation of explosive welding parameters and their effects on microhardness and shear strength, Mater. Design 24 (2005) 659-664.
[7] R. Mendes, J.B. Ribeiro, A. Loureiro, Effect of explosive characteristics on the explosive welding of stainless steel to carbon steel in cylindrical configuration, Mater. Design 51 (2013) 182-192.
[8] W.C. Jiang, B.Y. Wang, J.M. Gong, S.T. Tu, Finite element analysis of the effect of welding heat input and layer number on residual stress in repair welds for stainless steel clad plate, Mater. Design 32 (2011) 2851-2857.
[9] M. Sedighi, M. Honarpisheh, Experimental study of through-depth residual stress in explosive welded Al-Cu-Al multilayer, Mater. Design 37 (2012) 577-581.
[10] B. Mateša, D. Kozak, A. Stoić, I. Samardžić, The influence of heat treatment by annealing on clad plates residual stresses, Metalurgjia, 50 (2011) 227-230.
[11] R. Kaçar, M. Acarer, Microstructure-property relationship in explosively welded duplex stainless steel-steel, Mater. Sci. Eng. A 363 (2003) 290-296.
[12] M.E. Fitzpatrick, M.T. Hutchings, P.J. Withers, Separation of macroscopic, elastic mismatch and thermal expansion misfit stresses in metal matrix composite quenched plates from neutron diffraction measurements, Acta Mater. 45 (1997) 4867-4676.
[13] A. R. Pyzalla, Internal Stresses in Engineering Materials, in: W. Reimers, A. R. Pyzalla, A. Schreyer, H. Clemens (Eds.), Neutrons and Synchrotron Radiation in Engineering Materials Science, Wiley-VCH., Weinheim, 2008, pp. 21-56.
[14] J.W. Elmer, D.L. Olson, D.K. Matlock, The Thermal Expansion Characteristics of Stainless Steel Weld Metal, Weld. Res. Supp. 61 (1982) 293-301.